Parametric Study of Steel-Lined Pressure Shafts in Anisotropic Rock

Alexandre J. PACHOUD, Laboratory of Hydraulic Constructions (LCH), Ecole Polytechnique Fédérale de Lausanne (EPFL), Switzerland, Email : alexandre.pachoud@epfl.ch
Anton J. SCHLEISS, Laboratory of Hydraulic Constructions (LCH), Ecole Polytechnique Fédérale de Lausanne (EPFL), Switzerland, Email : anton.schleiss@epfl.ch

Topic: Planning and Designing Tunnels and Underground Structures

Summary: Steel-lined pressure tunnels and shafts are used to convey water from the reservoir to the turbines in high-head hydroelectric power plants. An axisymmetrical multilayer model is often considered by engineers for the design of the steel liner. Stresses and deformations can then be computed with a closed-form analytical solution in isotropic rock. When the rock is anisotropic, the lowest elastic modulus of the rock measured in situ is often considered in the analytical solution, which is regarded as conservative. In this work, the behaviour of steel liners in anisotropic rock was studied systematically by means of the Finite Element Method (FEM). The materials, namely steel, backfill concrete, near-field rock and far-field rock were modelled as linear and elastic, and a tied contact was assumed between the layers. The influence of geometrical and material parameters under a quasi-static internal water pressure was studied through an extensive parametric study. It was observed that, compared to the corresponding results in isotropic rock, maximum stresses in the steel-liner can be reduced up to 25% when anisotropy is considered. On the contrary, the maximum stresses in the far-field rock can be largely underestimated, namely up to 65%.

Keywords: *Pressure tunnels and shafts, Anisotropic rock, Steel liner, Stresses, Finite Element Method, Design*

1. Introduction

The development of high-capacity Pelton turbines and high-strength steel (HSS) allows the design of high-head power plants up to 2000m gross head to meet the increasing demand for peak energy [1]. With the rise of volatile new renewable energies, storage hydropower plants are subjected to more drastic operational requirements to balance the electricity grid. HSS has been developed to address the mechanical requirements, but they are more difficult to weld than ductile grades. Furthermore they are more sensitive to fatigue and brittle failure [2-3].

The common method for the design of steel-lined pressure tunnels and shafts considers an axisymmetrical model in isotropic rock to compute the stresses and deformations, taking the lowest elastic modulus measured in situ. Such an approach is commonly considered as conservative for the maximum stresses in the steel liner [4]. In Europe, the CECT (1980) recommendations [5] are followed for the design and the construction of steel-lined pressure tunnels and shafts. These guidelines are applicable for ductile steel grades, but are no longer adequate for the design with HSS. Instead, designers use a range of horizontal failure assessment methods and/or recommendations, but there is still a need for specific recommendations for steel-lined pressure shafts embedded in rock.

Several authors have studied the behaviour of linings in anisotropic rock (e.g. [6-11]). However, the case of steel-lined pressure tunnels or shafts has not yet been studied systematically in anisotropic rock. There is neither analytical solution nor extensive parametrical study of these structures available in anisotropic rock. In this work, the behaviour of steel liners considering the anisotropic behaviour of the rock is studied by means of the FEM. The solution in isotropic rock is introduced in Section 2. The constitutive models are discussed in Section 3. Finally, the numerical model, the parametric study and the results are presented in Section 4.

2. Solution in isotropic rock

2.1 Axisymmetrical model

The standard axisymmetrical model for the design of steel-lined pressure tunnels and shafts is introduced in Fig. 1.

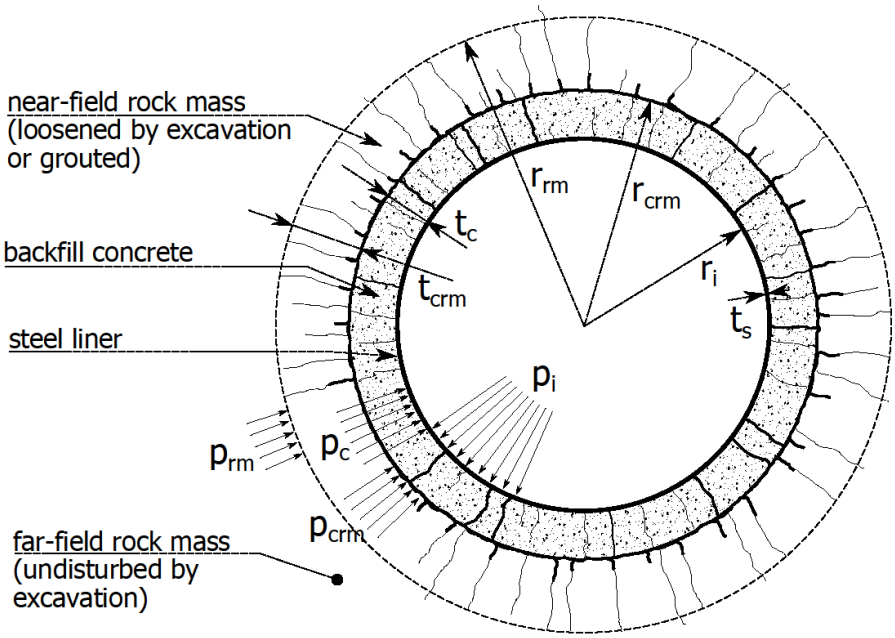

Fig. 1 *Axisymmetrical model for steel-lined pressure tunnels and shafts in isotropic rock*

In the multilayer model five zones are distinguished (e.g. [12-13]): (1) the steel liner; (2) an initial gap between the liner and the backfill concrete; (3) the backfill concrete; (4) the near-field rock; and (5) the far-field rock. All materials are considered linear elastic. The initial gap Δr_0 is an annular space between the steel liner and the backfill concrete due to the thermal shrinking of the steel during the first filling of the shaft. The backfill concrete is regarded as a radially cracked material due to its quasi-brittle nature. The near-field zone is a loosened zone of the rock resulting from the excavation method and the disturbance of the in situ stress field. Finally, the far-field rock is the undisturbed zone of the rock, assumed as homogeneous and isotropic in the axisymmetrical model.

2.2 Analytical solution

The model described in Fig. 1 has an analytical solution derived from the compatibility conditions on the displacements at the interfaces between the layers [14]. They can be written as

$$\begin{aligned} u_r^s(\mathrm{r}_c) - \Delta \mathrm{r}_0 &= u_r^c(\mathrm{r}_c)\,, \\ u_r^c(\mathrm{r}_{crm}) &= u_r^{crm}(\mathrm{r}_{crm})\,, \\ u_r^{crm}(\mathrm{r}_{rm}) &= u_r^{rm}(\mathrm{r}_{rm}) \end{aligned} \qquad (1)$$

where Δr_0 is positive, u_r denotes a radial displacement, and the superscripts and radii are related the layers accordingly to Fig. 1. Assuming that cracked materials cannot transmit tensile stresses and that the steel liner is modelled according to the thick-walled pipe theory [15], stresses and displacements can be derived analytically [13,14].

3. Constitutive models

3.1 Anisotropic rock

In the following a transversely isotropic rock is considered. Transverse isotropy is a particular case of orthotropy, i.e. with a plane of isotropy. Such a material can be described by five independent constants, namely the elastic moduli in the plane of isotropy and perpendicular to it respectively (E and E' respectively), the Poisson's coefficients which characterize the reduction in the plane of isotropy for the tension in the same plane and the tension in a direction normal to it respectively (ν and ν' respectively) and the shear modulus normal to the plane of isotropy (G') [16]. The shear modulus parallel to the plane of isotropy is computed as in an isotropic material with E and ν. G' can be computed by an empirical relation widely used in the literature:

$$G'_{emp} = \frac{E'}{1 + E'/E + 2\nu'} . \tag{2}$$

3.2 Cracked layers

To model the cracked layers (namely the backfill concrete and the near-field rock) a scalar damage parameter D_i is introduced as

$$1 - D_i = R_i \tag{3}$$

where i denotes a material parameter and R_i a scalar factor to be multiplied to a material property. Thus a radially damaged material has to be modelled. Since cylindrical coordinates are used, the elastic modulus should be drastically decreased in the tangential direction by a large factor as:

$$R_{E_\vartheta} = \tilde{E}_\vartheta / E_\vartheta \tag{4}$$

where the tilde symbol denotes a property of the damaged material and ϑ the tangential direction. Accordingly, the appropriate shear moduli and Poisson's ratios are decreased to account the effect of damage.

4. Systemic parametric study

4.1 Finite element model

The FEM code Mechanical APDL (ANSYS) 14.0 was used [17]. The FE model was built parametrically in order to run a parametric study using the Probabilistic Design System with a User-Defined Sampling. It assumes the same hypothesis than described in the analytical solution. An example of a mesh is shown in Fig. 2. The model is discretized in approximately 50'000 elements, depending on the generated parameters. The far-field rock is considered as infinite. It was taken into account by modelling a large far-field rock medium of $30 \cdot r_i$ starting from r_{rm}. Constitutive laws for the materials where implemented as described in Section 3.

Five material parameters have been assumed as constant, namely the steel properties ($E_s = 210$ GPa) and $\nu_s = 0.29$), the backfill concrete properties ($E_c = 20$ GPa and $\nu_c = 0.20$) and the Poisson's ratio of the near-field rock ($\nu_{crm} = 0.20$). In addition one geometrical parameter was considered as constant, namely the thickness of the backfill concrete ($t_c = 0.5$ m).

4.2 Variation of the parameters

There are 10 variables in the parametric model as defined in Table 1. A so-called reference set of cases is defined with given parameters as shown in Table 2. Starting from the reference set of cases, 7 parameters are changed individually as presented in Table 2. Within these sets of cases, 3

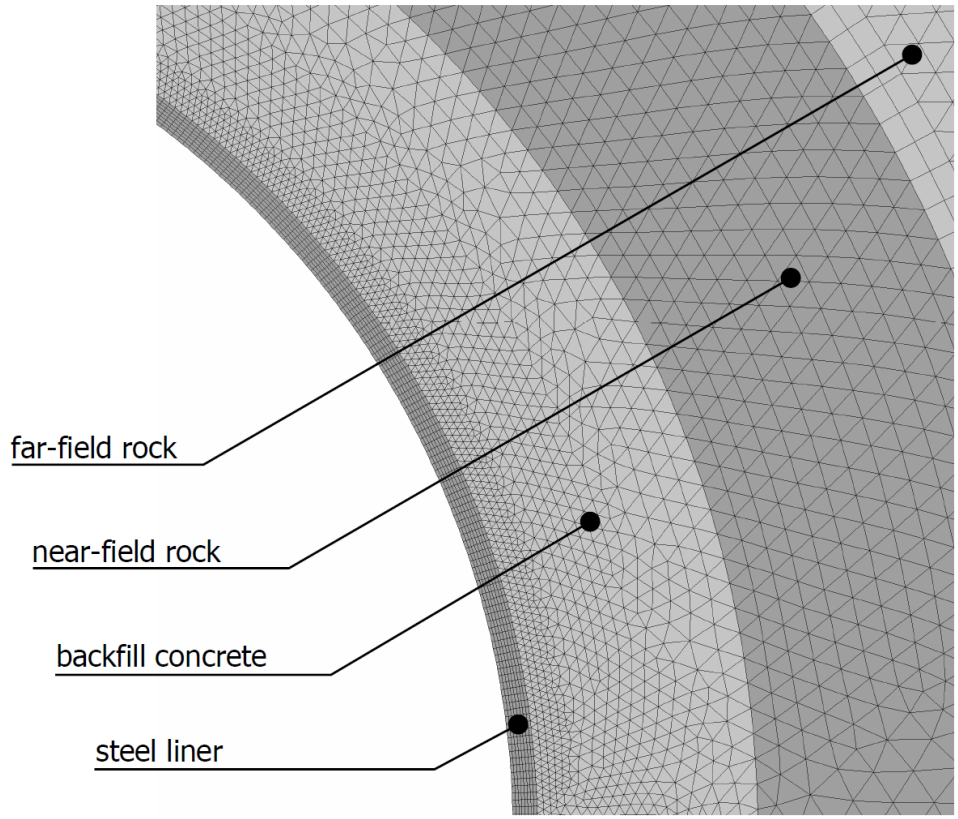

Fig. 2 *Example of a mesh of the FE model around the opening*

Table 1 *Definition of the variable parameters in the FE model*

Parameter	*Definition*
r_i	Internal radius of the steel liner
t_s	Thickness of the steel liner
t_{crm}	Thickness of the near-field rock (loosened)
p_i	Quasi-static internal water pressure
E, E', G', ν, ν'	Elastic properties of the transversely isotropic far-field rock (see Section 3.1)
E_{crm}	Elastic modulus of the near-field rock (loosened)

Table 2 *Variations of the parameters with respect to the reference set of cases*

Parameter	*Unit*	*Reference value*	*Value 1*	*Value 2*	*Value 3*
t_{crm}	m	0.5	1.0	2.0	3.0
E	GPa	10	1.0	15.0	25.0
G'/G'_{emp}	(-)	1.00	0.70	0.90	1.30
p_i	bar	150	50	100	200
ν	(-)	0.20	0.10	0.15	0.25
ν/ν'	(-)	1.30	1.20	1.80	2.50
E_{crm}/E'	(-)	0.80	0.70	1.00	1.30

parameters are changed accordingly to Table 3. Consequently, a total of 22 sets of cases were considered (7 x 3 + 1), each one containing 325 cases for a total of 7150 simulated cases. The parameters of each case respect the thermodynamic constraint of transversely isotropic materials and realistic practical ranges of variation (e.g. [16], [18]).

Table 3 *Variations of the variable parameters in each set of cases*

Parameter	*Unit*	*Minimum*	*Maximum*	*Increment*
r_i	m	1.00	3.00	0.50
t_s	m	0.015	0.055	0.010
E / E'	(-)	1.00	4.00	0.25

In addition, 5'000 isotropic cases were randomly sampled with a uniform distribution of the parameters in order to validate the FE model compared to the analytical solution (see Section 2.2). The results showed very good agreement.

4.3 Maximum stresses in the steel liner and in the far-field rock

For the following discussion, all the results are normalized. They are presented in a dimensionless form by dividing the numerical results of the anisotropic cases by the numerical results of the most conservative so-called corresponding isotropic cases. In the anisotropic case, the maximum first principal stresses in the steel liner always occur in the plane of isotropy. Denoting ϑ the angle with respect to the isotropic plane, the maximum normalized first principal stresses in the steel liner are thus computed as:

$$\hat{\sigma}^{s}_{1,\max} = \frac{\hat{\sigma}^{s}_{1,aniso}(\mathrm{r} = \mathrm{r}_i, \vartheta = 0)}{\hat{\sigma}^{s}_{1,iso}(\mathrm{r} = \mathrm{r}_i)} . \tag{5}$$

In the far-field rock, the maximum stresses do not occur at a constant angle of location, unlike in the steel liner, depending on the rock mass properties. The location of the maximum stresses is not discussed herein. The maximum normalized first principal stresses in the far-field rock are computed as:

$$\hat{\sigma}^{rm}_{1,\max} = \frac{\hat{\sigma}^{rm}_{1,aniso}(\mathrm{r} = \mathrm{r}_{rm}, \vartheta = \tilde{\vartheta})}{\hat{\sigma}^{rm}_{1,iso}(\mathrm{r} = \mathrm{r}_{rm})} \tag{6}$$

where $\tilde{\vartheta}$ denotes the direction of the maximum first principal stress for each case.

In Fig. 3(a), the influence of the near-field rock thickness on the maximum normalized first principal stresses in the steel liner is shown as a function of the degree of anisotropy. Results are lightened for reading purposes. The smaller the near-field rock thickness, the greater is the influence of the degree of anisotropy. Fig. 3(a) also shows that the greater the internal radius and the smaller the slenderness (i.e. t_s / r_i), the greater the influence of the degree of anisotropy. For all the tested cases, the maximum stresses were lower than in the corresponding isotropic case (normalized results lower than unity). The maximum stresses can be reduced up to 22% compared to the corresponding isotropic case for the tested cases.

In Fig. 3(b), the corresponding maximum normalized stresses in the far-field rock are presented. Small thickness of the near-field rock, small internal radius and great slenderness induce great influence of the degree of anisotropy. Unlike in the steel liner, the maximum first principal stresses in the far-field rock are up to 34% larger than in the corresponding isotropic case for the tested cases.

Fig. 4(a) illustrates the influence of the rock stiffness parallel to the plane of isotropy on the maximum stresses in the steel liner. The lower the stiffness, the lower is the influence of the degree of anisotropy.

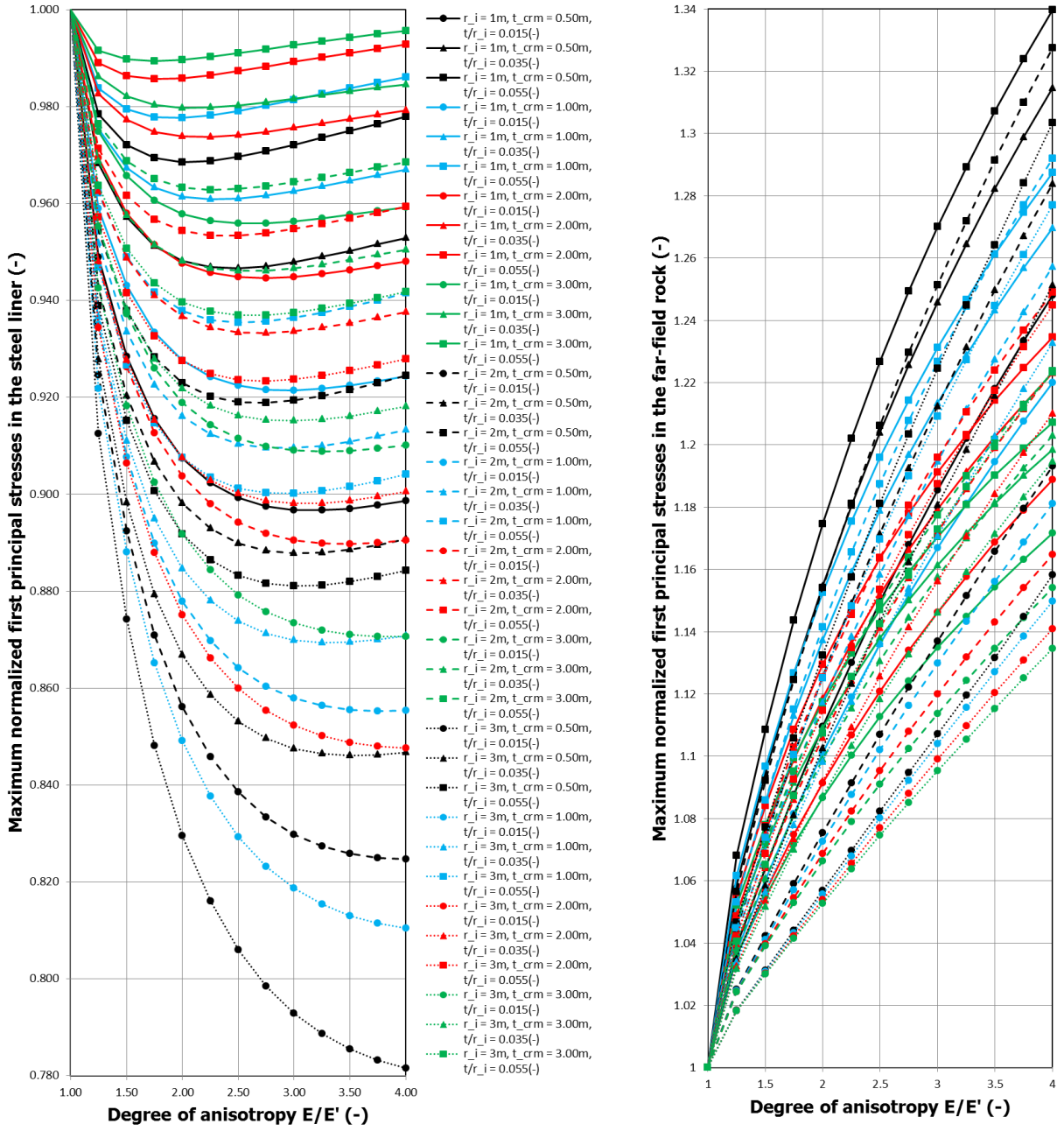

(a) In the steel liner *(b) In the far-field rock*

Fig. 3 *Maximum normalized first principal stresses in (a) the steel liner and in (b) the far-field rock as a function of the degree of anisotropy* E / E' *for different near-field rock thickness* t_{crm} *and by varying the slenderness* t_s / r_i *.* ***Black*** *refers to* t_{crm} *= 0.50 m,* ***blue*** *refers to* t_{crm} *= 1.00 m,* ***red*** *refers to* t_{crm} *= 2.00 m and* ***green*** *refers to* t_{crm} *= 3.00 m*

Indeed, in the case of a weak rock the participation of the concrete-rock system to withstand the internal pressure is low, and consequently anisotropy has a lower influence on the liner which takes a great part of the internal pressure. Similarly, the smaller the internal radius and the greater the steel thickness, the smaller is the influence of the anisotropy. This is also due to the fact that a stiffer liner is less influenced by changes in the rock mass modulus.

The corresponding maximum normalized stresses in the far-field rock are shown in Fig. 4(b). In a general manner, the greater the stiffness of the steel liner compared to the rock mass (i.e. low rock stiffness, low internal radius and great liner stiffness) the greater is the influence on the maximum stresses in the rock mass. Unlike the steel liner, the maximum stresses in the rock mass can be significantly increased compared to the corresponding isotropic case, up to 47% for the tested cases.

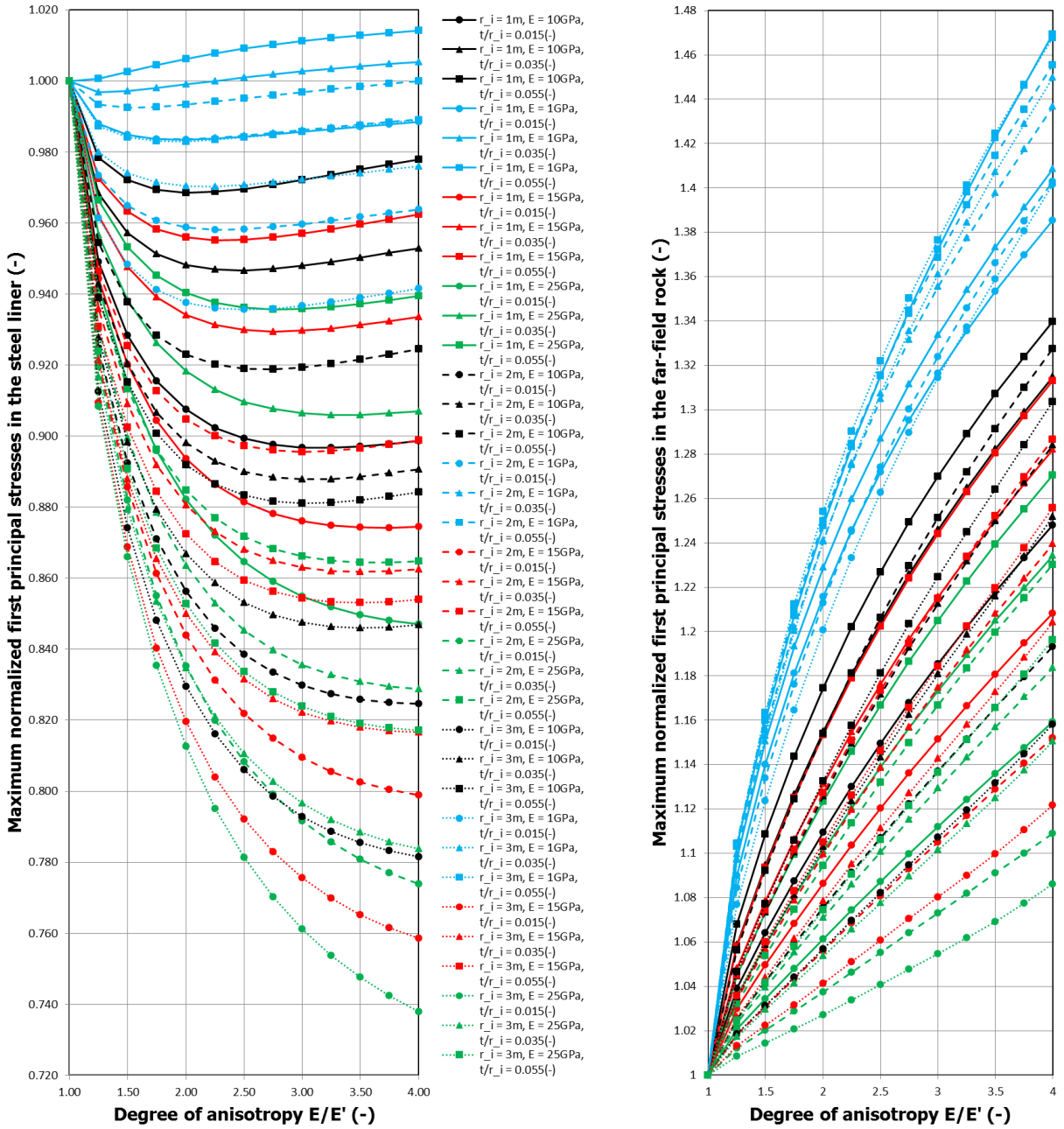

(a) In the steel liner *(b) In the far-field rock*

Fig. 4 *Maximum normalized first principal stresses in (a) the steel liner and in (b) the far-field rock as a function of the degree of anisotropy* E / E' *for different rock mass elastic modulus* E *and by varying the slenderness* t_s / r_i *.* ***Black*** *refers to* E *= 10 GPa,* ***blue*** *refers to* E *= 1 GPa,* ***red*** *refers to* E *= 15 GPa and* ***green*** *refers to* E *= 25 GPa*

Fig. 5(a) shows the influence of the deviation of the cross-shear modulus from the empirical relation (Eq. 2). The greater the cross-shear modulus compared to the empirical relation, the greater is the influence of the degree of anisotropy. For weak cross-shear modulus (e.g. 70% of the empirical relation in Fig. 5(a)) and for low degree of anisotropy, the maximum stresses in the steel liner are slightly higher than the corresponding isotropic cases. Otherwise the maximum stresses in the steel liner are generally lower than in the corresponding isotropic cases, down to 28% for the tested cases. Fig. 5(b) also illustrates that, the greater the slenderness of the steel liner, the lower is the influence of the anisotropy on the maximum stresses in the liner.

Fig. 5(b) illustrates the corresponding maximum normalized first principal stresses in the far-field rock. It can be observed that the influence of the degree of anisotropy is high for either low or

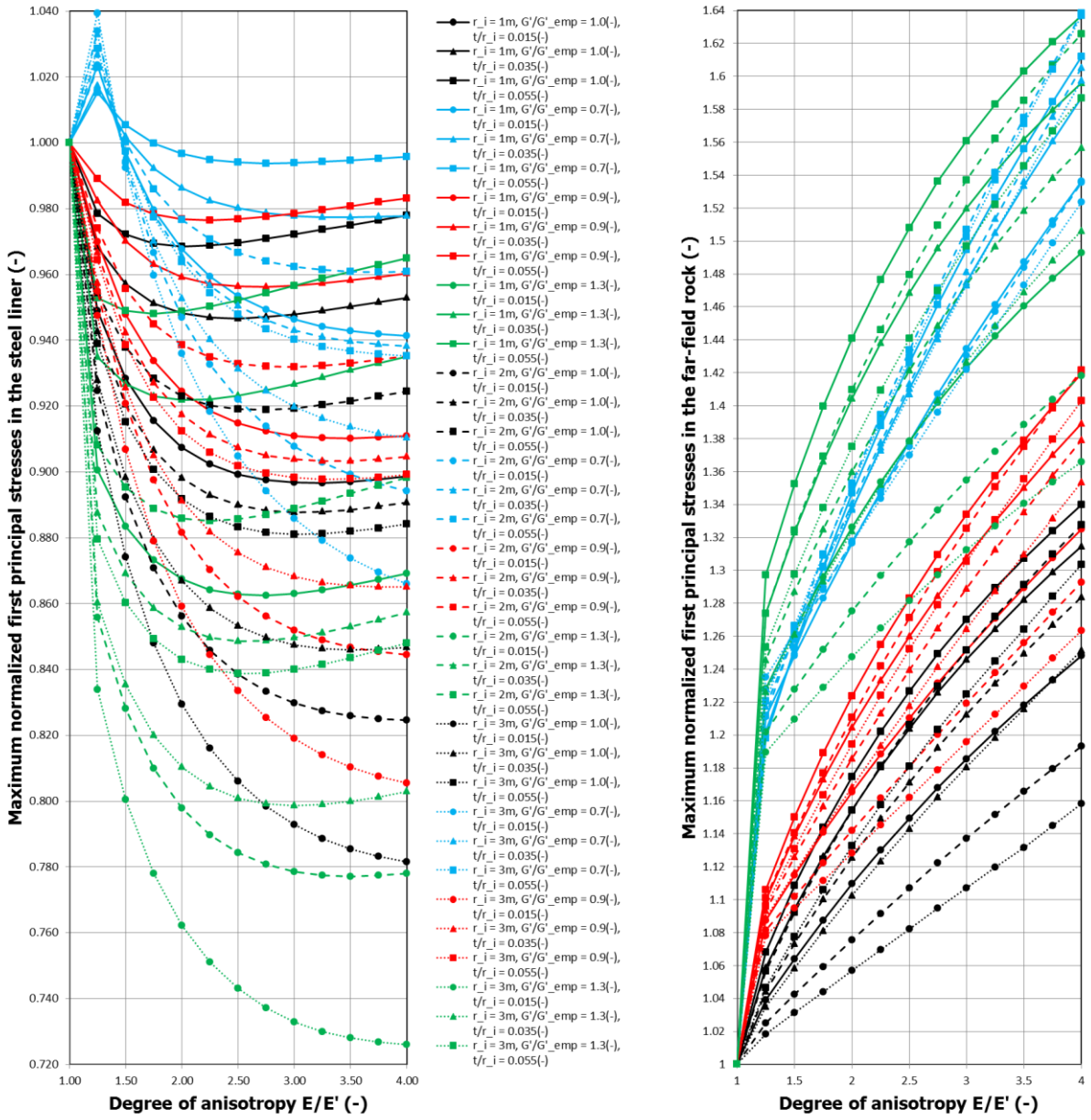

(a) In the steel liner *(b) In the far-field rock*

Fig. 5 *Maximum normalized first principal stresses in (a) the steel liner and in (b) the far-field rock as a function of the degree of anisotropy* E / E' *for different cross-shear modulus to empirical relation ratio* G'/G'_{emp} *and by varying the slenderness* t_s / r_i *. **Black** refers to* G'/G'_{emp} *= 1.0 (-), **blue** refers to* G'/G'_{emp} *= 0.7 (-), **red** refers to* G'/G'_{emp} *= 0.9 (-) and **green** refers to* G'/G'_{emp} *= 1.3 (-)*

high values of the cross shear-modulus (e.g. 70 or 130% of the empirical relation in Fig. 5(b)). For medium values (e.g. 90 or 100%), the influence is lower, although significant. Maximum stresses in the far-field rock can be up to 64% higher than in the corresponding isotropic case.

5. Conclusions

For the design of steel-lined pressure tunnels and shafts, an axisymmetrical model with the smallest rock mass modulus observed in situ is often considered as conservative in terms of maximum stresses in the steel liner. The anisotropy is not commonly taken into account since the mechanical behaviour of the steel-concrete-rock system is still not well understood.

In this work, the behaviour of steel-lined pressure tunnels and shafts in anisotropic rock was studied by means of the FEM. The rock mass was assumed as transversely isotropic. An extensive parametric study was performed over 10 variable material and geometrical parameters. Maximum

stresses in the steel liner and in the far-field rock were illustrated and trends of behaviour were outlined.

When considering anisotropic rock behaviour, the maximum first principal stresses in the steel liner are lower than in the corresponding isotropic case that would be considered for the design. They can be reduced down to 25% for the tested cases. Considering isotropic rock with the lowest rock mass modulus is thus a conservative assumption in terms of maximum stresses in the steel liner.

Unlike the steel liner, considering an isotropic case is not conservative in terms of maximum first principal stresses in the far-field rock, which can be up to 65% greater than the prediction considering isotropic rock. Maximum stresses in the rock are thus underestimated.

The presented results allow a better understanding of the mechanical behaviour of steel-lined pressure tunnels and shafts in anisotropic rock. This is an important issue in the view of optimized design guidelines for steel-lined pressure tunnels using high-strength steel, which are sensitive to fatigue and brittle failure issues.

Acknowledgements

This study is part of the research project consortium HydroNet 2: Modern methodologies for design, manufacturing and operation of hydropower plants, funded by the Swiss Competence Center Energy and Mobility (CCEM-CH) and Swisselectric Research.

References

[1] Schleiss, A. J. and Manso, P. A. (2012). Design of pressure relief valves for protection of steel-lined pressure shafts and tunnels against buckling during emptying. Rock Mechanics and Rock Engineering 45(1):11-20.
[2] Cerjak H. and Enzinger, N. and Pudar, M. (2013). Development, experiences and qualifications of steel grades for hydro power conduits. In: Proceedings of the Conference on High Strength Steels for Hydropower Plants, Graz University of Technology, Graz, Austria.
[3] Greiner, R. and Innerhofer sen, G. and Stering, W. (2013). New design aspects for steel linings of pressure shafts made of high strength steel. In: Proceedings of the Conference on High Strength Steels for Hydropower Plants, Graz University of Technology, Graz, Austria.
[4] Brekke, T. L. and Ripley, B. D. (1987). Design guidelines for pressure tunnels and shafts. Tech. rep., University of California at Berkeley, Department of Civil Engineering, Berkeley, California 94707, EPRI AP-5273, Project 1745-17.
[5] CECT. (1980). Recommendations for the design, manufacture and erection of steel penstocks of welded construction for hydropower installations. European Committee of Boiler, Vessel and Pipe Work Manufacturers.
[6] Éristov, V. S. (1967a). Computation of pressure tunnel linings in anisotropic rocks. Hydrotechnical Construction 1(5):436-442.
[7] Éristov, V. S. (1967b). Experimental studies of pressure-tunnel linings in anisotropic formations. Hydrotechnical Construction 1(12):1054-1057.
[8] USACE (1997). Tunnels and shafts in rock (EM 1110-2-2901). U.S. Army Corps of Engineers.
[9] Baslavskii, I. A. (1973). Stresses in the lining of a pressure tunnel driven in an inhomogeneous rock mass. Soviet Mining 9(6):613-617.
[10] Postol'skaya, O. K. (1986). Effect of the structure of a rock mass and properties of rocks on the stress state of hydraulic pressure tunnels. Hydrotechnical Construction 20(1):25-30.
[11] Kumar, P. and Singh, B. (1990). Design of reinforced concrete lining in pressure tunnels, considering thermal effects and jointed rock mass. Tunnelling and Underground Space Technology 5(1/2):91-101.
[12] ASCE (2012). Steel Penstocks, Manuals and Reports on Engineering Practice, vol 79. American Society of Civil Engineers, Reston, Virginia.
[13] Schleiss, A. J. (1988). Design criteria applied for the lower pressure tunnel of the North Fork Stanislaus River hydroelectric project in California. Rock Mechanics and Rock Engineering 21(3):161-181.
[14] Hachem, F. E. and Schleiss, A. J. (2011). A review of wave celerity in friction-less axisymmetrical steel-lined pressure tunnels. Journal of Fluids and Structures 27(2):311-328.
[15] Timoshenko, S. P. and Goodier, J. N. (1970). Theory of elastic stability, 3rd edn. McGraw-Hill

International.
[16] Amadei, B. and Savage W. Z. and Swolfs, H. S. (1987). Gravitational stresses in anisotropic rock masses. International Journal of Rock Mechanics and Mining Sciences 24(1):5-14.
[17] ANSYS Inc (2011). ANSYS® Academic Research, Help System, Documentation Release 14.0. ANSYS Inc.
[18] Amadei, B. and Swolfs, H. S. and Savage, W. Z. (1988). Gravity-induced stresses in stratified rock masses. Rock Mechanics and Rock Engineering 21(1):5-14.